

PACS: 81.10.-h; 42.70.-a

ISSN 1729-4428

K. Balakrishnan¹, S. Sakthy Priya^{1,2}, A. Lakshmanan^{1,3}, P. Surendran^{1,4}, Karthik Kannan⁵,
P. Geetha⁶, G. Vinitha⁷, P. Praveen Kumar⁸, P. Rameshkumar^{8*}

Studies on structural, optical nonlinearity and antibacterial activity of Piperazine (bis) p-toluenesulfonate single crystal for optical limiting and biological applications

¹PG and Research Department of Physics, Nehru Memorial College (Autonomous), Affiliated to Bharathidasan University,
Puthanampatti 621 007, India

²Department of Physics, Arignar Anna Government Arts College, Namakkal 637 002, Tamilnadu, India

³Department of Physics, MAM College of Engineering, Siruganur, Tiruchirappalli 621 102, Tamilnadu, India

⁴Department of Physics, Government Arts and Science College, Komarapalayam 638 183, Tamilnadu, India

⁵Chemical Sciences Department and the Radical Research Center, Ariel University, Ariel 40700, Israel

⁶Department of Physics, Quaid-E-Millath Government College for Women (Autonomous), Chennai 600 002, Tamilnadu, India

⁷Division of Physics, School of Advanced Sciences, VIT Chennai 600127, Tamil Nadu, India

⁸Department of Physics, Presidency College (Autonomous), Chepauk, Triplicane, Chennai 600005, Tamilnadu, India,
rameshkumarevr@gmail.com

Piperazine (bis) p-toluenesulfonate (PPTSA), an organic single crystal was synthesized and grown at environmental temperature by slow evaporation process using methanol as the solvent. The grown PPTSA crystal is from the *triclinic* system and belongs to the space group $P\bar{1}$. Powder X-ray diffraction was performed to ensure lattice parameters. Analysis and confirmation of functional groups and bonds were carried out through FT-IR spectral study. The optical characteristics were investigated using the UV-Vis spectrum such as the optical absorption, cut-off wavelength were calculated. The photoluminescence investigation was conducted to assess the luminous characteristics of grown crystal. The calculated NLO parameters like β , n_2 , and $\chi^{(3)}$ were found to be 0.0495×10^{-4} (cm/W), 8.705×10^{-10} (cm²/W), 5.316×10^{-7} (esu) and Optical Limiting threshold value was found to be 3.074×10^{-3} (Wcm⁻²). Antibacterial studies were carried out to investigate the biological significance against selected foodborne germs.

Keywords: Crystal growth, optical material, optical limiting, antibacterial activity.

Received 23 August 2022; Accepted 30 January 2023.

Introduction

Nonlinear optical (NLO) materials received a lot of attention over decades owing to the numerous uses in photonics, such as light-emitting diodes, telecommunication system, high data storage, optical switching and drug delivery [1-3]. Organic nonlinear optical material researches have gained significant attention owing to its usage in optical devices. They have considerable optical susceptibilities and an inherent quick response time as compared to inorganic compound.

Because of the delocalized electrons at π - π^* orbitals, organic materials are anticipated to have rather significant nonlinear optical characteristics. This anticipation motivates the considerable search among organic crystals for improved NLO materials. When compared to inorganic materials, NLO chromophores are implanted in organic materials in a noncentrosymmetric way, revealing excellent nonlinear activity [3-6]. Tosylic acid, also known as p-toluene sulfonic acid, is an organic acid available in solid phase. Charge transfer has been achieved due to the presence of CH₃ group as an electron donor and

sulfonate group serves as an acceptor in the title compound. Complexes including organic and inorganic bases that may aid in the induction of high NLO behavior [7-10]. On the other side of NLO materials, organic molecules with full conjugated bonds agree to form a group. Over the previous two decades, The NLO features of big organic molecules have been the subject of considerable research. Piperazine is an aromatic ring where nitrogen atoms are located in 1, 4 of the ring that makes up an organic molecule [11].

The grown PPTSA crystal was studied by powder X-ray diffraction (PXRD), FTIR, optical absorption, photoluminescence, and Z-scan analysis. Furthermore, the grown crystal was tested for antibacterial activity against some bacterial species.

I. Experimental procedures

1.1. Materials synthesis and crystal growth

PPTSA title crystal was grown by conventional slow evaporation method from the purchased chemicals piperazine and p-toluenesulfonic acid in 1:1 equimolar ratio taking methanol as solvent at ambient temperature. Fig. 1 depicts the chemical reaction process of the produced PPTSA substance. After dissolving the reactants in methanol, the mixture was stirred for 6 hours using a magnetic stirrer to achieve homogeneous solution before being filtered through standard filter paper. The impurities-free saturated solution was wrapped with a perforated sheet and allowed to evaporate in a dust-free environment. The grown crystal was reaped after a span of four weeks and harvested crystal in depicted in Fig. 2.

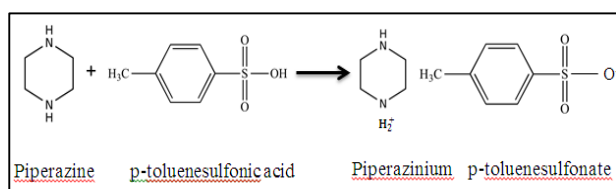


Fig. 1. Reaction scheme of PPTSA.

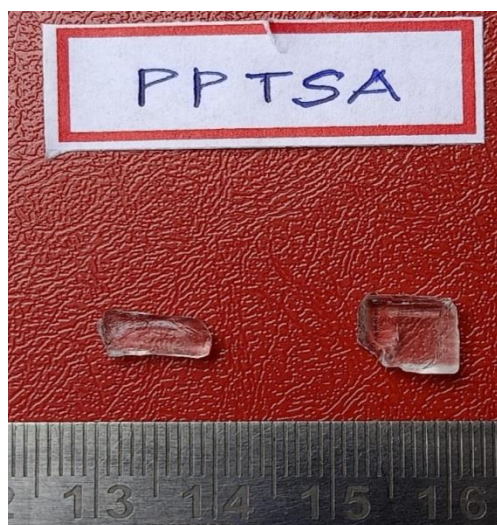


Fig. 2. Photograph of the grown PPTSA single crystal.

1.2. Instrumentation

Investigation of crystal structure was performed by an

XPRT-PRO powder X-ray diffractometer with CuK α radiation ($\lambda=1.5406 \text{ \AA}$, 0.1 min^{-1} , 10° to 80°). Perkin-Elmer (model: Spectrum Two) FTIR spectrophotometer with KBr pellet, the presence of chemical bonding and vibrational modes in the title sample PPTSA were affirmed. The spectra showing optical absorption were recorded using a Perkin Elmer UV-Visible spectrometer (model: Lambda 35) with a wavelength range of 190–1100 nm. The spectra of luminescence were captured using a spectrofluorophotometer (Shimadzu/RF6000) with a xenon lamp as the excitation of cause. Under CW laser (532 nm) stimulation, optical characteristics of nonlinear third-order were determined using a Z-scan experiment. The disc diffusion technique was used to explore the biological activity against chosen bacterial species.

II. Results and discussion

Fig. 3 depicts the powder X-ray diffraction pattern of grown PPTSA crystal. This experiment validated the triclinic crystal structure with the space group $P\bar{1}$ and lattice factors $a = 5.9644 \text{ \AA}$, $b = 13.1731 \text{ \AA}$, $c = 13.5968 \text{ \AA}$, and $V = 934.32 \text{ \AA}^3$, which are similar to the published values Table 1 [12, 13].

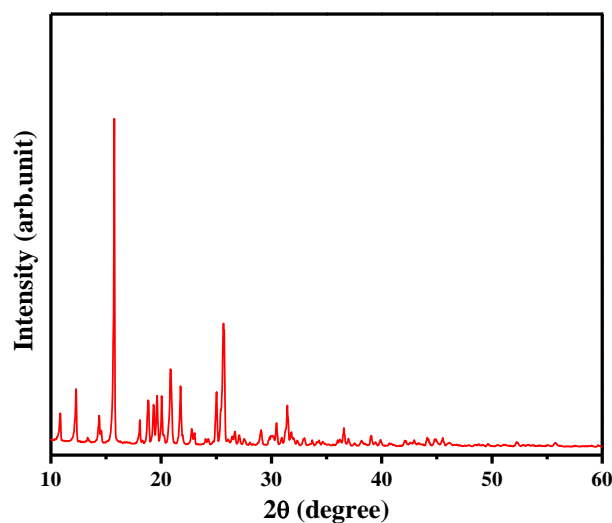


Fig. 3. X-ray diffraction pattern of PPTSA crystal.

$$D = (k\lambda/\beta\cos\theta) \quad (1)$$

$$\beta \cos\theta = \frac{k\lambda}{D} + 4\eta \sin\theta \quad (2)$$

The micro strain (η) in the grown PPTSA crystal's lattice was estimated using the Hall-Williamson equation $\beta \cos\theta = 4\eta\sin\theta + k\lambda/D$. The slope plotted between $\beta \cos\theta$ versus $4\sin\theta$ as depicted in Fig. 4. The existence of tensile strain in the developed crystal is indicated by a positive strain value 6.70×10^{-4} of the grown PPTSA crystal.

$$\delta = \frac{1}{D^2} \quad (3)$$

The dislocation density (δ) influences the characteristics of the crystal and its value is $3.4408 \times 10^{14} \text{ (lines/m}^2\text{)}$ [14].

Table 1.

Crystallographic data for PPTSA single crystal

Parameters	Present work	Reported reference [13]
Unit cell dimensions	a= 5.9644 Å b= 13.1731 Å c= 13.5968 Å $\alpha= 73.680^\circ, \beta = 110.310^\circ,$ $\gamma = 83.390^\circ$	a= 5.9697 Å b= 13.1609 Å c= 13.6027 Å $\alpha= 73.665^\circ, \beta = 110.2650^\circ,$ $\gamma = 83.348^\circ$
Volume	V= 934.32 Å ³	V= 1017.71 Å ³
Space group	P $\bar{1}$	P $\bar{1}$
System	Triclinic	Triclinic
Crystallite Size (D) nm	53.91 nm	
Dislocation Density (δ)	3.4408×10^{14} lines/m ²	

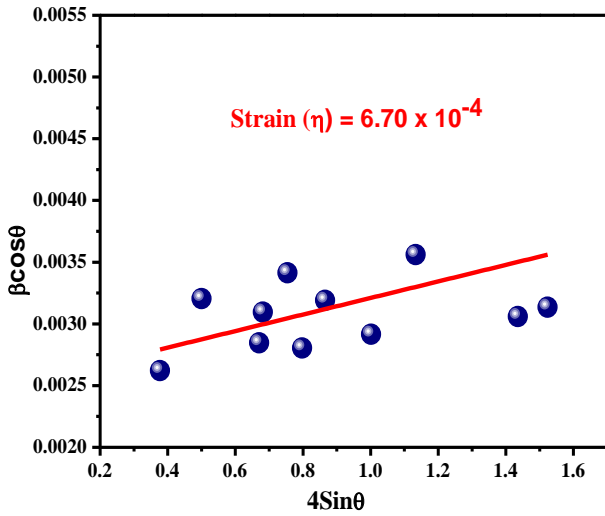


Fig. 4. Williamson-Hall plot of PPTSA crystal.

Fig. 5 displays FT-IR spectrum of grown PPTSA crystal. The N-H stretching of piperazine ions corresponds to vibrations at 3435 cm⁻¹ [15]. The peaks at 3001 cm⁻¹ and 2753 cm⁻¹ suggest the absorption of C-H symmetric and asymmetric bending vibration. The peak of p-toluenesulfonic acid C=C-H stretching mode is 3001 cm⁻¹. Bands at 2816 and 2753 cm⁻¹ suggest attenuation of the C-H stretching mode. The minor peak at 1916 cm⁻¹ is due to the aromatic overtones of p-toluenesulfonic acid [16-17]. The NH₂⁺ deformation is responsible for the peaks at 1624 and 1558 cm⁻¹. At 1459 cm⁻¹, the C=C stretching phase occurred. The peak of the N-H asymmetric bending vibration is 1495 cm⁻¹. Stretching of CH₂ has a peak at 1439 cm⁻¹. At 1396 cm⁻¹, the sulphonate group revealed its stretching vibration. The peak at 1380 cm⁻¹ is caused by CH₂ deformation. The asymmetric and symmetric stretching peaks for the C-N group were 1317 and 1189 cm⁻¹, correspondingly. The C-H group's in-plane and out-of-plane bending modes were 1085 and 737 cm⁻¹, respectively [18]. Table 2 lists all of the wavenumbers as well as the functional groups to which they belong.

The fundamental and crucial quality for piezoelectric, photonic and electro-optic materials is the transparent nature of the formed crystal in the whole spectrum. Electronic transitions in the crystal PPTSA could be understood when incident radiation interacts with the grown crystal. Light absorption allows electrons for the transition in σ and π orbitals from the lower to the higher

energy states. For laser frequency conversion applications, optical transmission window, cut-off wavelength and absorption peak are critical characteristics [19]. The absorption spectrum of PPTSA has been recorded and the lower cut-off wavelength was recorded as 305 nm and no absorbance was found beyond this limit that is displayed in Fig. 6. The suggested value of lower cut-off wavelength should lie between 200-400 nm which could be suitable for the fabrication of laser diodes. The electronic excitations between N and H atoms in piperazine cause the cut-off. The low optical absorption value in the whole visible band implies that grown PPTSA crystals are suited for the production of nonlinear optical systems. The formula is used to calculate the band gap [20],

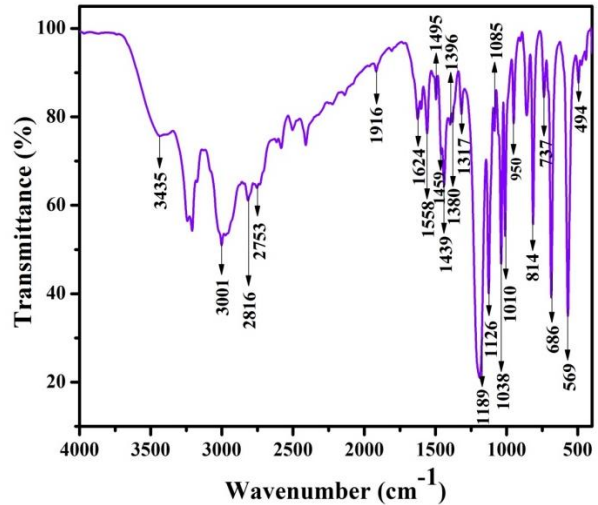


Fig. 5. FTIR spectrum of PPTSA crystal.

$$E_g = \frac{1240}{\lambda} eV \quad (4)$$

It is determined to be 4.06 eV. The measured spectra and band gap value accord well with the published value. The increased optical transmittance might be owing to fewer flaws, which raises the output intensity. This is more appropriate for NLO applications. The optical absorption co-efficient on photon energy could be calculated using the equation below [21],

$$\alpha = \frac{2.3026}{t} \log_{10} \left(\frac{100}{T} \right) \quad (5)$$

Table 2.

Vibration wavenumbers and their associated assignments of PPTSA title compound	
Wavenumber (cm ⁻¹)	Assignments
3435	N-H stretching
3001	C=C-H symmetric stretching mode
2816	C-H stretching mode
2753	Asymmetric stretching vibrations
1916	p-toluenesulfonic acid
1624	NH ₂ ⁺ deformation
1558	NH ₂ ⁺ deformation
1495	N-H asymmetric bending vibration
1459	C=C stretching
1439	Stretching of CH ₂
1396	Stretching vibration
1380	CH ₂ deformation
1317	C-N group's asymmetric
1189	Symmetric stretching
1126	Asymmetric stretching vibrations of the C-C group
1085	C-H group's in-plane bending modes
1038	C-C group's bending vibration
1010	C-S stretching vibration
950	S-O-C stretching vibration
814	p-toluenesulfonic acid
737	Symmetric and out-of-plane bending modes
686	N-H wagging vibration
596	C-C-N deformations
494	C-N-C deformations

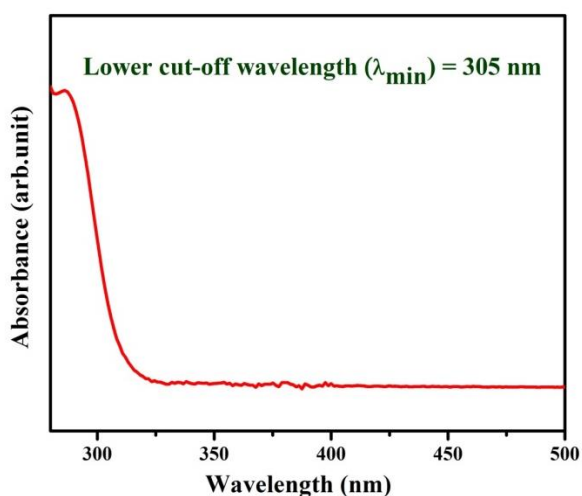


Fig. 6. Absorption spectrum of PPTSA crystal.

Where t is the sample thickness and T is the transmittance (percent). The energy band gap values was calculated using standard relation [22],

$$(\alpha h\nu)^2 = A(h\nu - E_g)^n \quad (6)$$

Where E_g indicates the band gap and A indicates the constant. The band gap values are determined by plotting against $(\alpha h\nu)^2$ versus $h\nu$, as shown in Fig. 7, and it is 4.06 eV. The theoretically computed band gap value agrees with the observed value. The band gap of the PPTSA crystal demonstrates its better visible field properties.

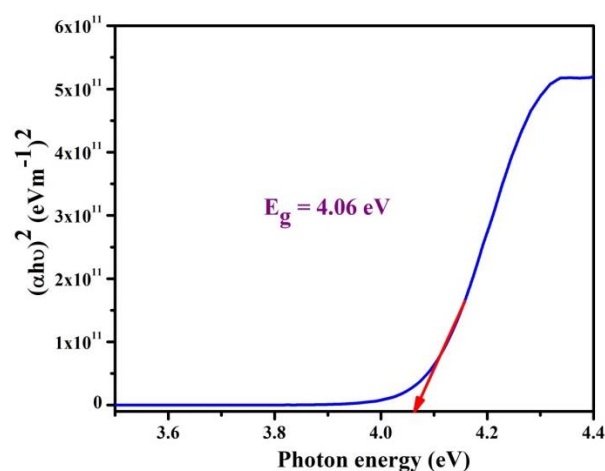


Fig. 7. Tauc's plot of PPTSA crystal.

Fluorescence is vital in medical and scientific studies in aromatic compounds or with many conjugated double bonds that have a high degree of permanence [23]. Good quality of crystal can be analyzed with this instrumentation. The inherent properties of the crystal like crystalline nature, dislocations, structural arrangement and impurities are attributed with the intensity of the emission spectra of the sample [24]. The Photoluminescence spectrum was recorded with the aid of spectrofluorometer for the grown title compound PPTSA and depicted in Fig. 8. When the sample was stimulated with 280 nm, the spectra illustrate a wide elevation pinpointed at 571 nm, indicating yellow radiation. The increased intensity of emission can be used to detect organic organisms. The inclusion of electron-donating group NH and electron-drawing carboxylic group which might increase electron

mobility would result in greater PL emission.

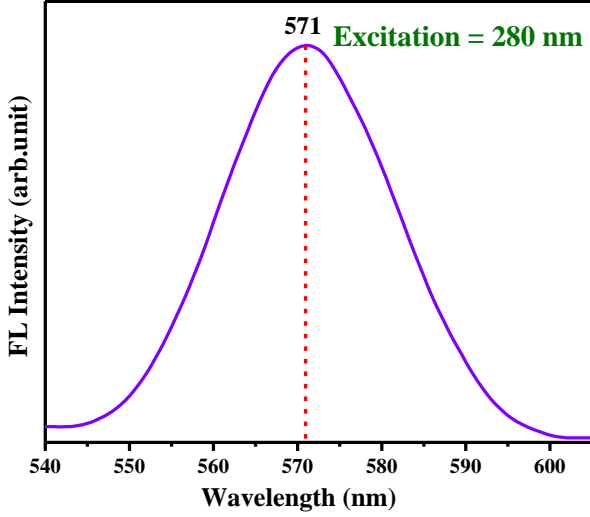


Fig. 8. Luminescence spectra of PPTSA crystal.

The third-order NLO characteristics of PPTSA sample were studied by Z-scan measurements to calculate the nonlinear absorption co-efficient (β), refractive index (n_2), and susceptibility ($\chi^{(3)}$) [25-28]. CW laser (532 nm) with a laser intensity of 100 mW was employed. The title crystal was attached to 90° and displaced along the negative axis. The propagation direction is along the -Z to +Z axis. The sample table can be translated in a variety of ways. Each movement is precisely controlled by a computer. The sample's transmitted intensity was measured and it is sensed by light detector and quantified.

The predicted intensity in a closed aperture (CA) is proportional to the aperture radius (2 mm) and remains

constant throughout the operation. Using an open aperture (OA) approach, intensity was directly recorded by placing a lens in front of the detector to determine the nonlinear absorption co-efficient (β) and an aperture was located between the lens and the front of the detector to determine NLR (n_2). Fig. 9 (a & b) shows the PPTSA crystals CA and OA Z-scan curves, respectively. The refractive index of the grown crystal and their absorption nature directly affect the power of a laser beam. According to the NLR values, the sample generates further focusing or defocusing. The samples CA pattern demonstrates self-defocusing behavior. The OA pattern exhibits reverse saturable absorption. Third-order NLO parameters were calculated using the standard relation [29]. β was determined using OA readings as follows,

$$\beta = \frac{2\sqrt{2}\Delta T}{I_0 L_{\text{eff}}} (m/w) \quad (9)$$

The following equation estimates the samples susceptibility.

$$\chi^{(3)} = \sqrt{(R_e \chi^{(3)})^2 + (I_m \chi^{(3)})^2} \quad (10)$$

Where the components in the expression are given as

$$R_e(\chi^{(3)}) = \frac{10^{-4} \varepsilon_0 c^2 n_0^2 n_2}{\pi} (cm^2/W) \quad (11)$$

$$I_m(\chi^{(3)}) = \frac{10^{-2} \varepsilon_0 c^2 n_0^2 \lambda \beta}{4\pi^2} (cm/W) \quad (12)$$

Where ε_0 (8.854×10^{-12} F/m), n_0 and c are obvious notations. The calculated NLO susceptibility value was found to be 5.316×10^{-7} (esu). Table 3 shows the third-order NLO parameters for the grown PPTSA crystal. The

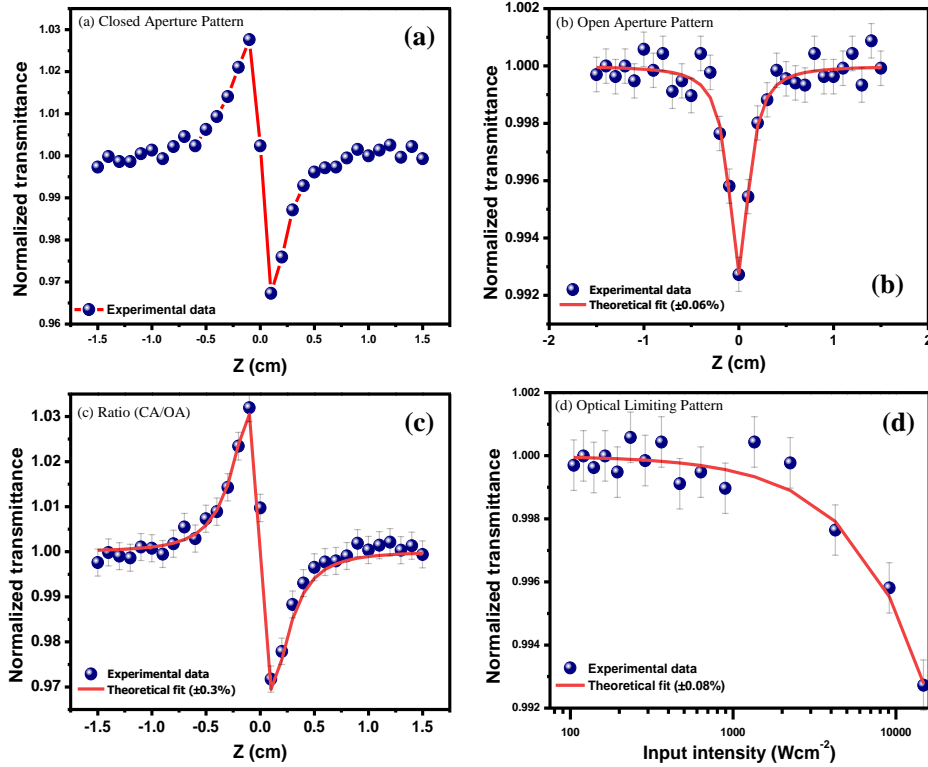


Fig. 9. (a) Closed aperture, (b) Open aperture, (c) Ratio of closed to open aperture z-scan and (d) Optical limiting pattern of PPTSA sample.

material's nonlinear optical properties indicate that it might be employed in optoelectronics devices such as optical limiting, night vision devices, and light emitting diode applications.

The variation of normalized transmittance with respect to the input intensity of laser beam has been displayed in Fig. 9d, is known as optical limiting curve which is plotted from the data extracted from open aperture scan. The plot suggests that the normalized transmittance is linear at low input intensity when the intensity starts increasing at one particular intensity the nonlinearity arises called as onset limiting threshold. The normalized transmittance approaches minimum at $Z=0$. The limiting threshold intensity is found different for different input intensities. This investigation is a valuable tool to fabricate optical limiting devices. The synthesized single crystal has been acknowledged as a potential candidate for optical limiting applications.

In recent years researchers focus on the biomedical

applications in addition to the NLO applications, one among them is antibacterial activity. The titular compound PPTSA was examined against human pathogens gram +Ve (*Klebsiella pneumoniae*, *Escherichia coli*), and gram -Ve (*Streptococcus aureus*, *Streptococcus Pneumoniae*) through disc diffusion method. The observed inhibition zones in the diffusion plate have been displayed in Fig. 10. Zone of inhibition for evaluating antibacterial activity was taken in the order 40, 50, and 60 μ L respectively in which the grown PPTSA shows an excellent response 24.5 mm (60 μ L) against gram negative *Streptococcus aureus*. This result ensures concentration makes significant impact on inhibition zone (Table 4). As a matter of fact commercially available amoxicillin shows only 15 mm (60 μ L). Characteristics such as intermolecular interaction, solubility, and conductivity may be important in antibacterial activity. Investigating the title compound's for antibacterial properties has demonstrate that the existence of hydrogen bonding interactions boost

Table 3.

NLO parameters of the grown PPTSA single crystal	
Third-order NLO parameters	Values
Laser wavelength	532 (nm)
Focal length of lens used	130 (mm)
Radius of aperture used	1.5 (mm)
Radius of the beam on aperture	3 (mm)
Intensity of the laser at the focus	0.01478 (MW/cm ²)
Reighley range (Z_R)	1.271 (mm)
Nonlinear absorption coefficient (β)	$0.0495 \times 10^{-4} \text{ cm/W}$
Nonlinear refractive index (n_2)	$8.705 \times 10^{-10} \text{ cm}^2/\text{W}$
Real part of the third order susceptibility [$R_e(\chi^{(3)})$] cm^2/W	$2.039 \times 10^{-7} \text{ esu}$
Imaginary part of the third order susceptibility [$I_m(\chi^{(3)})$] cm/W	$4.910 \times 10^{-7} \text{ esu}$
Third order nonlinear optical susceptibility [$\chi^{(3)}$]	$5.316 \times 10^{-7} \text{ esu}$
Optical Limiting threshold values (OL)	$3.074 \times 10^{-3} (\text{Wcm}^{-2})$

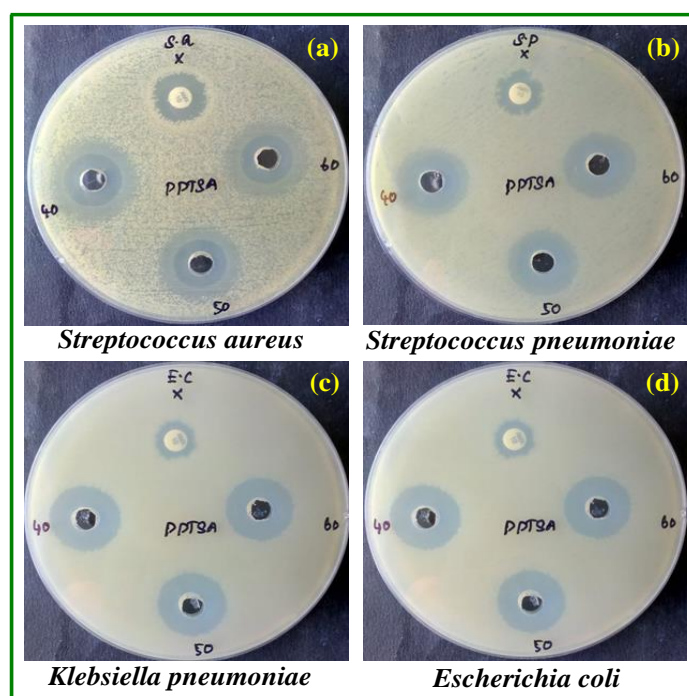


Fig. 10. Antibacterial plate photos of the grown PPTSA crystal (a) *Streptococcus aureus*, (b) *Streptococcus pneumoniae*, (c) *Klebsiella pneumoniae* and (d) *Escherichia coli*.

Table 4

The antibacterial activity of PPTSA single crystal

Test microorganism	Gram reaction	Zone of inhibition (mm)			
		40 (μ L)	50 (μ L)	60 (μ L)	Amx (μ L)
<i>Klebsiella pneumoniae</i>	G+	21	21	22	16
<i>Escherichia coli</i>	G+	19	19	19	11
<i>Streptococcus aureus</i>	G-	24	23	24	15
<i>Streptococcus Pneumoniae</i>	G-	20	20	20	13

antibacterial effectiveness significantly [31-35]. Furthermore, the presence of a free HNCCO moiety promotes the delocalization of π -electrons over the PPTSA molecule, increasing lipophilicity [36]. The enhancement of lipophilicity of the compound retards the normal cell processes via degradation of cell's permeability in turn pathogens are made destroyed. Hence the titular compound could be an effective material for bio medical applications [37-40].

Conclusions

Piperazine (bis) p-toluenesulfonate (PPTSA) crystals were successfully grown at ambient temperature using a slow evaporation approach. Crystallinity of the crystal was confirmed with PXRD and crystallizes *triclinic* and belong to $P\bar{1}$. The functional groups of PPTSA crystal was affirmed by FTIR spectra. The UV-Vis spectrum reveals that the energy band gap value is 4.06 eV. The photoluminescence measurements confirmed that the produced crystal could be used to fabricate LEDs. The grown PPTSA crystal exhibits RSA and self-defocusing nature which are inevitable for optical limiting and switching applications. The title crystal PPTSA was

subjected to antibacterial activity against human pathogen and found that it is a efficient material for drug manufacturing.

Acknowledgements

One of the authors P. Surendran is grateful to UGC-NFHE [F1-17.1/2015-16/NFST-2015-17-ST-TAM-1335] and A. Lakshmanan wish to thank the UGC-RGNF [F1-17.1/2016-17/RGNF-2015-17SC-TAM-21802] New Delhi, India, for the financial support.

Conflicts of interest

We declare that we have no conflicts of interest.

Balakrishnan K. – Ph.D Research Scholar;
Sakthy Priya S. – Ph.D in Physics, Guest Lecturer;
Lakshmanan A. – Ph.D in Physics, Assistant Professor;
Surendran P. – Ph.D in Physics, Guest Lecturer;
Kannan Karthik – Ph.D in Physics, Postdoctoral Fellow;
Geetha P. – Assistant Professor;
Vinitha G. – Assistant Professor;
Kumar P. Praveen – Associate Professor;
Rameshkumar P. – Assistant Professor.

- [1] E. Selvakumar, G. Anandha babu, P. Ramasamy, Rajnikant, T. Uma Devi, R. Meenakshi, A. Chandramohan, *Synthesis, growth, structure and spectroscopic characterization of a new organic nonlinear optical hydrogen bonding complex crystal: 3-Carboxyl anilinium p-toluene sulfonate*, Spectrochim. Acta Part A Mol. Biomol. Spectrosc. 125, 114 (2014); <https://doi.org/10.1016/j.saa.2014.01.035>.
- [2] K. Sangeetha, S. Thamocharan, R.R. Babu, S.M. Kumar, *Linear and nonlinear optical properties of 4-nitrobenzoic acid (4-NBA) single crystals*, Bull. Mater. Sci. 41, 73 (2018); <https://doi.org/10.1007/s12034-018-1583-5>.
- [3] R. Aarthy, P. Umarani, C.R. Raja, *Interpretation of molecular structure and third-order nonlinear optical studies of 4-methylbenzylammonium nitrate single crystal*, Appl. Phys. A. 124, 498 (2018); <https://doi.org/10.1007/s00339-018-1913-x>.
- [4] G. Peramaiyan, R.M. Kumar, G. Bhagavannarayana, *Crystal growth, structural, optical and dielectric studies of ammonium p-toluenesulfonate*, J. Cryst. Growth. 408, 14 (2014); <https://doi.org/10.1016/j.jcrysgro.2014.09.011>.
- [5] V. Thayanithi, P.P. Kumar, *Growth, optical, mechanical and thermal behavior of unidirectionally grown L-Glutaminium p-Toluenesulfonate crystal*, Mater. Res. Express. 6, 46207 (2019); <https://doi.org/10.1088/2053-1591/aafd43>.
- [6] S. Sagadevan, P. Murugasen, *Studies on Optical, Mechanical and Electrical Properties of Organic Nonlinear Optical p-Toluidine p-Toluenesulfonate Single Crystal*, J. Cryst. Process Technol. 4, 99 (2014); <https://doi.org/10.4236/jcpt.2014.42013>.
- [7] C. Amirthakumar, B. Valarmathi, I.M. Zahid, G. Vinitha, V. Seetharaman, A. Ramnathan, R.M. Kumar, *Studies on the third order nonlinear optical properties of a novel o-Phenylenediaminium p-Toluenesulfonate single crystal*, Mater. Lett. 247, 25 (2019); <https://doi.org/10.1016/j.matlet.2019.03.068>.
- [8] G. Shanmugam, S. Brahadeeswaran, *Spectroscopic, thermal and mechanical studies on 4-methylanilinium p-toluenesulfonate – a new organic NLO single crystal*, Spectrochim. Acta - Part A Mol. Biomol. Spectrosc. 95, 177 (2012); <https://doi.org/10.1016/j.saa.2012.04.100>.

- [9] M. Suresh, S. Asath Bahadur, S. Athimoolam, *Synthesis, growth and characterization of a new hydrogen bonded organic tosylate crystal: l-alaninium p-toluenesulfonate for second order nonlinear optical applications*, J. Mater. Sci. Mater. Electron. 27, 4578 (2016); <https://doi.org/10.1007/s10854-016-4334-7>.
- [10] R. Kaliammal, S. Sudahar, G. Parvathy, K. Velsankar, K. Sankaranarayanan, *Physicochemical and DFT studies on new organic Bis-(2-amino-6-methylpyridinium) succinate monohydrate good quality single crystal for nonlinear optical applications*, J. Mol. Struct. 1212, 128069 (2020); <https://doi.org/10.1016/j.molstruc.2020.128069>.
- [11] A. Rathika, M. Antony Lilly Grace, A. Arun Kumar, R. Subramaniyan, R. Suja, *Organic piperazine p-nitrophenol (PPN) single crystal growth and characterization*, Mater. Today Proc. 47, 4741 (2021); <https://doi.org/10.1016/j.matpr.2021.05.663>.
- [12] A. Suvitha, P. Vivek, P. Murugakoothan, *Nucleation kinetics, growth and characterization of guanidinium 3-nitrobenzoate single crystal*, Opt. - Int. J. Light Electron Opt. 124, 3534 (2013); <https://doi.org/10.1016/j.ijleo.2012.10.069>.
- [13] P. Rekha, G. Peramaiyan, M. NizamMohideen, R. Mohan Kumar, R. Kanagadurai, *Synthesis, growth, structural and optical studies of a novel organic Piperazine (bis) p-toluenesulfonate single crystal*, Spectrochim. Acta Part A Mol. Biomol. Spectrosc. 139, 302 (2015); <https://doi.org/10.1016/j.saa.2014.12.069>.
- [14] S. Sakthy Priya, K. Balakrishnan, P. Surendran, A. Lakshmanan, S. Pushpalatha, G. Ramalingam, P. Rameshkumar, K. Kaviyarasu, T. Ashok Hegde, G. Vinitha, *Investigations on structural, electrical, and third order nonlinear optical properties of benzimidazolium maleate single crystal*, Mater. Today Proc. 36, 163 (2021); <https://doi.org/10.1016/j.matpr.2020.02.680>.
- [15] R.U. Mullai, S.R. Kanuru, R. Arul Jothi, S. Gopinath, S. Vetrivel, *Synthesis, growth, thermal, mechanical and optical studies of piperazinium based cupric sulfate (PCS) single crystals: A third order nonlinear optical material*, Opt. Mater. (Amst). 110, 110482 (2020) <https://doi.org/10.1016/j.optmat.2020.110482>.
- [16] S. Gunasekaran, B. Anita, *Spectral investigation and normal coordinate analysis of piperazine*, Indian J. Pure Appl. Phys. 46, 833 (2008); <http://nopr.niscair.res.in/handle/123456789/3024>.
- [17] S. Chinnasami, M. Manikandan, S. Chandran, R. Paulraj, P. Ramasamy, *Growth, Hirshfeld surfaces, spectral, quantum chemical calculations, photoconductivity and chemical etching analyses of nonlinear optical p-toluidine p-toluenesulfonate single crystal*, Spectrochim. Acta Part A Mol. Biomol. Spectrosc. 206, 340 (2019); <https://doi.org/10.1016/j.saa.2018.08.015>.
- [18] R.R. Kumar, P. Sathya, R. Gopalakrishnan, *Structural, vibrational, thermal and optical studies of organic single crystal: Benzotriazolium p-toluene sulfonate (BTPTS)*, in: AIP Conf. Proc., 20508 (2016); <https://doi.org/10.1063/1.4946559>.
- [19] S.V. Ashvin Santhia, B. Aneeba, S. Vinu, R. Sheela Christy, A.M. Al-Mohameed, D.A. Al Farraj, *Studies on physicochemical and antibacterial deeds of amino acid based L-Threonium sodium bromide*, Saudi J. Biol. Sci. 27, 2987 (2020); <https://doi.org/10.1016/j.sjbs.2020.09.020>.
- [20] S.S.B. Solanki, R.N. Perumal, T. Suthan, *Growth and characterization of propyl 4-hydroxybenzoate single crystal by vertical Bridgman technique*, Mater. Res. Innov. 22, 144 (2018); <https://doi.org/10.1080/14328917.2016.1266428>.
- [21] G. Feng, L. Li, D. Xu, *Optical Properties of CaNb₂O₆ Single Crystals Grown by OF*, Crystals. 11, 928 (2021); <https://doi.org/10.3390/cryst11080928>.
- [22] A.T. Ravichandran, R. Rathika, M. Kumaresavanji, *Growth and Z-scan analysis of semi-organic Bis(picolinic acetate) Zinc(II) single crystal for third order NLO applications*, J. Mol. Struct. 1224, 129048 (2021); <https://doi.org/10.1016/j.molstruc.2020.129048>.
- [23] V. Subhashini, S. Ponnusamy, C. Muthamizhchelvan, B. Dhanalakshmi, *Growth and characterization of piperazinium 4-nitrophenolate monohydrate (PNP): A third order nonlinear optical material*, Opt. Mater. (Amst). 35, 1327 (2013); <https://doi.org/10.1016/j.optmat.2013.01.032>.
- [24] G. Anandha Babu, P. Ramasamy, *Growth and characterization of 2-amino-4-picolinium toluene sulfonate single crystal*, Spectrochim. Acta Part A Mol. Biomol. Spectrosc. 82, 521 (2011); <https://doi.org/10.1016/j.saa.2011.08.003>.
- [25] V. Siva, S. Asath Bahadur, A. Shameem, A. Murugan, S. Athimoolam, M. Suresh, *Synthesis, supramolecular architecture, thermal and optical behavior of 4-methoxyanilinium perchlorate: A promising third-order NLO material for optical limiting device applications*, Opt. Mater. (Amst). 96, 109290 (2019); <https://doi.org/10.1016/j.optmat.2019.109290>.
- [26] V. Siva, A. Shameem, A. Murugan, S. Athimoolam, M. Suresh, S. Asath Bahadur, *A promising guanidinium based metal-organic single crystal for optical power limiting applications*, Chinese J. Phys. 64, 103 (2020) <https://doi.org/10.1016/j.cjph.2020.01.001>.
- [27] A. Anandhan, C. Sivasankari, M. Saravanabhavan, V. Siva, K. Senthil, *Synthesis, crystal structure, spectroscopic investigations, physicochemical properties of third-order NLO single crystal for optical applications*, J. Mol. Struct. 1203, 127400 (2020); <https://doi.org/10.1016/j.molstruc.2019.127400>.
- [28] K. Pichan, S.P. Muthu, R. Perumalsamy, *Crystal growth and characterization of third order nonlinear optical piperazinium bis(4-hydroxybenzenesulphonate) (P4HBS) single crystal*, J. Cryst. Growth. 473, 39 (2017); <https://doi.org/10.1016/j.jcrysgro.2017.05.018>.

- [29] S. Kamaal, M. Mehkoom, M. Muslim, S.M. Afzal, A. Alarifi, M. Afzal, A. Alowais, M. Muddassir, A.N. Albalwi, M. Ahmad, *Crystal Structure, Topological and Hirshfeld Surface Analysis of a Zn(II) Zwitterionic Schiff Base Complex Exhibiting Nonlinear Optical (NLO) Properties Using Z-Scan Technique*, Crystals. 11, 508 (2021); <https://doi.org/10.3390/cryst11050508>.
- [30] K. Nivetha, K. Aravinth, K. Senthil, S. Kalainathan, *Evaluation of structural, spectral, thermal and optical properties of an efficient centrosymmetric organic single crystal 2-[2-(4-diethylamino-phenyl)-vinyl]-1-methyl pyridinium tetrafluoroborate for nonlinear optical applications*, J. Mol. Struct. 1225, 129082 (2021); <https://doi.org/10.1016/j.molstruc.2020.129082>.
- [31] M. Tamil Elakkiya, K. Anitha, *CCDC 1541880: Experimental Crystal Structure Determination*, Mater. Lett. 235, 202 (2019); <https://doi.org/10.1016/j.matlet.2018.10.015>.
- [32] S. Sakthy Priya, K. Balakrishnan, P. Surendran, A. Lakshmanan, S. Pushpalatha, P. Rameshkumar, P. Geetha, K. Kannan, T.A. Hegde, G. Vinitha, *Investigation on nonlinear optical and antibacterial properties of organic single crystal: p-Toluidinium L-Tartrate*, Chem. Data Collect. 31, 100640 (2021); <https://doi.org/10.1016/j.cdc.2020.100640>.
- [33] V. Revathi, K. Karthik, H. Mahdizadeh, *Antibacterial activity and physico-chemical properties of metal-organic single crystal: Zinc (Tris) thiourea chloride*, Chem. Data Collect. 24, 100279 (2019); <https://doi.org/10.1016/j.cdc.2019.100279>.
- [34] S.S. Priya, K. Balakrishnan, P. Surendran, A. Lakshmanan, P. Geetha, P. Rameshkumar, T.A. Hegde, G. Vinitha, A.A. Raj, *Investigations on Structural, Mechanical, Optical, Electrical, Third-Order Nonlinear Optical and Antibacterial Activity of 4-Aminopyridine Monophthalate Single Crystal*, J. Electron. Mater. 50, 291 (2021); <https://doi.org/10.1007/s11664-020-08497-w>.
- [35] K. Kannan, D. Radhika, S. Vijayalakshmi, K.K. Sadasivuni, A. A. Ojiaku, U. Verma, *Facile fabrication of CuO nanoparticles via microwave-assisted method: photocatalytic, antimicrobial and anticancer enhancing performance*, Int. J. Environ. Anal. Chem. 102, 1095 (2022); <https://doi.org/10.1080/03067319.2020.1733543>.
- [36] G.B. Dani RK, P.R. Srivastava M, Y.R. Gondwal M, *Synthesis, Characterization, Single Crystal Structural Studies, Antibacterial Activity and DFT Investigations of 2-Chloro-5-Ethoxy-3,6- Bis(Methylamino)-1,4-Benzoquinone*, Pharm. Anal. Acta. 6, 1 (2015); <https://doi.org/10.4172/2153-2435.1000418>.
- [37] V. Beena, S. Ajitha, S.L. Rayar, C. Parvathiraja, K. Kannan, G. Palani, *Enhanced Photocatalytic and Antibacterial Activities of ZnSe Nanoparticles*, J. Inorg. Organomet. Polym. Mater. 31, 4390 (2021); <https://doi.org/10.1007/s10904-021-02053-7>.
- [38] P. Surendran, A. Lakshmanan, S.S. Priya, K. Balakrishnan, P. Rameshkumar, K. Kannan, P. Geetha, T.A. Hegde, G. Vinitha, *Bioinspired fluorescence carbon quantum dots extracted from natural honey: Efficient material for photonic and antibacterial applications*, Nano-Structures and Nano-Objects. 24, 100589 (2020); <https://doi.org/10.1016/j.nanoso.2020.100589>.
- [39] K. Kannan, D. Radhika, D. Gnanasangeetha, S.K. Lakkaboyana, K.K. Sadasivuni, K. Gurushankar, M.M. Hanafiah, *Photocatalytic and antimicrobial properties of microwave synthesized mixed metal oxide nanocomposite*, Inorg. Chem. Commun. 125, 108429 (2021); <https://doi.org/10.1016/j.inoche.2020.108429>.
- [40] A. Lakshmanan, P. Surendran, S. Sakthy Priya, K. Balakrishnan, P. Geetha, P. Rameshkumar, T.A. Hegde, G. Vinitha, K. Kannan, *Investigations on structural, optical, dielectric, electronic polarizability, Z-scan and antibacterial properties of Ni/Zn/Fe₂O₄ nanoparticles fabricated by microwave-assisted combustion method*, J. Photochem. Photobiol. A Chem. 402, 112794 (2020) <https://doi.org/10.1016/j.jphotochem.2020.112794>.

К. Балакрішнан¹, С. Сакті Прія^{1,2}, А. Лакшманан^{1,3}, П. Сурендран^{1,4},
Картік Каннан⁵, П. Гіта⁶, Г. Вініта⁷, П. Правін Кумар⁸, П. Рамешкумар^{8*}

Дослідження структурної, оптичної нелінійності та антибактеріальної активності монокристалу піперазину (bis) р-толуолсульфонату для оптичних обмежень та біологічних застосувань

¹Університет Бхаратідасану, Путанампатті, Індія;

²Урядовий коледж мистецтв Арігнар Анна, Намаккал, Тамілнад, Індія;

³Інженерний коледж МАМ, Сіруганур, Тіручіраппаллі, Тамілнад, Індія;

⁴Державний коледж мистецтв і науки, Комарапалаям, Тамілнад, Індія;

⁵Відділ хімічних наук і Центр радикальних досліджень, Аріельський університет, Аріель, Ізраїль;

⁶Державний жіночий коледж Куейд-І-Міллат (автономний), Тамілнад, Індія;

⁷Школа передових наук, VIT Ченнай, Таміл Над, Індія;

⁸Президентський коледж (автономний), Ченапак, Триплікан, Ченнай, Тамілнад, Індія, rameshkumarevr@gmail.com

Органічний монокристал піперазин (bis) р-толуолсульфонат (PPTSA) синтезовано і вирощено при температурі навколишнього середовища шляхом процесу повільного випаровування із використанням метанолу у якості розчинника. Вирощено кристал PPTSA відноситься до *триклінної* системи і належить до просторової групи P1. Для перевірки параметрів ґратки застосовано метод порошкової рентгенівської дифракції. Аналіз і конформацію функціональних груп і зв'язків проводили за допомогою спектрального дослідження FT-IR. Оптичні характеристики досліджено із використанням спектру UV-Vis, зокрема, досліджено оптичне поглинання, розрахована довжина хвилі відсікання. Для оцінки світлових характеристик вирощеного кристала досліджено спектри фотолюмінесценції. Розраховані параметри NLO, такі як β , n_2 та $\chi^{(3)}$, були встановлені, відповідно, як 0.0495×10^{-4} (cm/W), 8.705×10^{-10} (cm²/W), 5.316×10^{-7} (esu), виявлене порогове оптичне обмеження склало 3.074×10^{-3} (Wcm⁻²). Здійснено антибактеріальні дослідження для вивчення біологічної активності проти вибраних мікробів харчового походження.

Ключові слова: вирощування кристалів, оптичний матеріал, оптичне обмеження, антибактеріальна дія.